ARL-RR-6 PT I

AR-008-363

AD-A268 730

DEPARTMENT OF DEFENCE

DEFENCE SCIENCE AND TECHNOLOGY ORGANISATION

AERONAUTICAL RESEARCH LABORATORY

MELBOURNE, VICTORIA

Research Report 6
Part I

A BENCHMARK BENDING TEST OF A THICK SPECIMEN
PART I - EXPERIMENTS

by

J.M. FINNEY
E. KOWAL

Approved for public release.

JUNE 1993

AR-008-363

DEPARTMENT OF DEFENCE
DEFENCE SCIENCE AND TECHNOLOGY ORGANISATION
AERONAUTICAL RESEARCH LABORATORY

Research Report 6
Part I

A BENCHMARK BENDING TEST OF A THICK SPECIMEN
PART I - EXPERIMENTS

by

J.M. FINNEY
E. KOWAL

SUMMARY

An experiment has been undertaken to provide benchmark data for validating methods of calculating the plastic behaviour of metals. In this experiment a 30 mm square-test-section specimen of 7050-T7451 aluminium alloy has been loaded in four-point bending, and the surface distortions of all four faces have been measured with the aid of a square grid pattern imposed on the surfaces before deformation. This part of the Report describes the experimental details and gives the results of the material property tests, thus providing sufficient information for the prediction of surface displacements. Part II of the Report gives the measured displacements with which predictions may be compared.

DSTO
AUSTRALIA

POSTAL ADDRESS: **Director, Aeronautical Research Laboratory, 506 Lorimer Street, Fishermens Bend, 3207 Victoria, Australia.**

TABLE OF CONTENTS

Page Nos.

1. INTRODUCTION

Modern numerical techniques can be used to analyse such complex geometries and loadings that the mind may be swayed by such power to think that the results invariably describe reality. It is obviously essential that, from time to time, numerical results should be validated against those from experiment. One area requiring the application of numerical analysis is metal fatigue. Here the applications range from a determination of residual stress patterns for various life enhancement techniques to an evaluation of the stresses around the tip of a growing crack. In one form or another plasticity is involved, and the plastic region is usually localized and undergoes cyclic reversals in sign. In such a situation the precise description of the plastic behaviour can significantly influence the numerical results.

To demonstrate the potential of any numerical procedure for a complex situation it must be capable of accurate prediction in a simpler situation. In relation to the cyclic plasticity just mentioned, where strains may be 10% or even much greater, it would seem reasonable to require of any numerical procedure that it should accurately predict behaviour under similar monotonic strains. To this end a bending test on a thick square-section aluminium alloy specimen has been devised to give strains typical of those in cyclic plasticity. Coupled with tensile test results on the same material sufficient information is available for numerical techniques to predict the surface displacements of the test section.

Given that marked anticlastic curvature may occur in thick sections under large-strain bending it was thought that the prediction of surface displacements would be a good test for numerical analyses. This report is in two parts. Part I presents the experimental details and tensile results to enable numerical prediction, and Part II gives the experimentally-determined surface displacements.

2. SCOPE

The bending specimen was deformed in a four-point loading jig to two levels of bending moment. Before deformation a square grid pattern of 2 mm spacing was applied to each of the four faces of the test section and it is the deformation of the grid patterns that defines the surface displacements. Rigid body displacements were not measured.

Five tensile specimens were tested to obtain the yield stress and work hardening behaviour of the material. Stress relaxation was found to be quite substantial and the tensile specimens were also used to measure this phenomenon at three nominal strain levels. The significance of the stress relaxation was that the grid pattern deformations were obtained by measuring surface replicas which take time to set, and it was important to record the grid patterns when the stress and strain were stable.

Stress relaxation may add a complexity to numerical prediction. If such analysis can cope with this phenomenon there will be a greater confidence in being able to predict cyclic plasticity, given that practical fatigue cycling is not normally at a constant rate and often involves periods of rest. The approach then is to make available tensile and stress relaxation data for the material, and the test geometry and loads for the bending specimen, thus providing information for the numerical prediction of the surface displacements of the bend specimen.

3. MATERIAL AND TEST MACHINE

All specimens were machined from a 144 mm thick rolled plate of 7050-T7451 aluminium alloy. (Though of little concern to the present work, the material is that from which certain fuselage bulkheads are made for the F/A-18 fighter aircraft). The longitudinal axis of all specimens was that of the rolled plate. They were taken from different locations through the thickness of the plate but there was no evidence that the properties were affected by the location. Table 1(a) gives the tensile properties of the material as determined by the manufacturer.

A 250 kN servohydraulic test machine was used for all tests. The tension and stress relaxation tests were controlled from a clip gauge mounted on the specimen, and the bending tests were controlled from strain gauges mounted outside the test section in the nominally-elastic region. Load cell readings, actuator displacements, and strain gauge outputs were recorded with respect to time, as well as load versus displacement.

4. TENSILE AND STRESS RELAXATION TESTS

The specimens for determining the tensile and stress relaxation behaviour of the material are illustrated in Fig.1. The clip gauge controlling the tests was mounted centrally in the parallel test section. One test was made to a total strain of 0.12 under a continuous ramp rate of 0.04 per minute, after which the stress relaxation behaviour was determined. Several other specimens were strained to a value of 0.04 which was kept constant for several hours to obtain stress relaxation data, then strained to a level of 0.08, then to 0.12, each time allowing relaxation. The same strain ramp rate of 0.04 per minute was used for each strain increment.

Figure 2 illustrates the average stress/strain curve obtained from some of the relaxation tests and from this curve the proof stresses have been obtained and are recorded in Table 1(b). Table 2 lists the average stress/strain data for nominal strains up to 12%. Characterization of the plastic flow is obviously of considerable importance in numerical modelling and the various stress-strain curves obtained experimentally have been averaged and the Ramberg-Osgood power law [1] used to describe the relationship, as follows:

$$\varepsilon = \sigma/E + K(\sigma/E)^n$$

where ε is the nominal strain (defined as the fractional change in length)

σ is the nominal stress (i.e. based on original area)

E is the tensile modulus, value = 71.0 GPa

K is a constant, value = 10 exp 87.54

n is a constant exponent, value = 41.70

Figure 2 also gives the plot of this equation and demonstrates the quality of the characterization.

The stress relaxation data are given in Table 3 for nominal strains of 0.04, 0.08 and 0.12, and they are also plotted in Fig. 3. Excellent representation of each data set was obtained with a least-squares best-fit second-degree polynomial as can be seen in Fig. 3. The average best-fit curve for each strain level is plotted in Fig. 4 and the equations characterizing each curve are given in Table 4. These equations can be used to determine the relaxed stress at any time for strains within the range tested, and should be accurate enough for extrapolating to strains and times a little outside those used experimentally.

5. BENDING TEST

5.1 Specimen and test details

The bending specimen has a nominal 30 mm x 30 mm square test section, and its geometry is shown in Fig. 5 which also includes the dimensions of the bending jig. Figure 6 shows the specimen in the test machine before loading and illustrates the location of some of the strain gauges controlling the test. Strain gauges were mounted on both top and bottom surfaces and connected to the strain control console of the test machine. The specimen/jig contact points were liberally coated with grease and the specimen was given a strain ramp until a certain force was reached at which point the output of the strain gauges was held constant. The time to reach the pre-determined load was approximately two minutes. At this stage relaxation was allowed to occur for a period of about 22 hours (after which time the load was virtually constant), and replicas of the four deformed surfaces were taken under load.

The total replication time was approximately 90 minutes after which the whole procedure was repeated, the only change being that the strain ramp rate was slower than previously, and was such that the next level of pre-determined load was reached also in approximately two minutes. The various times and loads achieved are given in Table 5. It is emphasised that at no time was the specimen unloaded; the output of the strain gauges was either a ramp with time or was held constant. This procedure is illustrated in Fig. 7.

5.2 Grids and replication

A grid pattern was applied to each of the four faces of the test section by a photoresist technique [2]. In the present application the four surfaces of the test section were polished flat to a 3 micron finish and the photoresist material was sprayed on. The square grid spacing was nominally 2 mm and the section of the grid pattern which was central in the test section on each face, and which measured nominally 28 mm by 28 mm, covered the area used for the displacement measurements. Figure 8 shows photographs of the grids on the specimen.

Replicas of the grid patterns used a silicone-based precision impression material* with enough activator to give hardening in about 15 to 20 minutes. The material has a low enough viscosity to be syringeable and it was forced into perspex holders clamped to the specimen until the holders were completely filled. The replicating material was left in the holders after hardening to give it support and make it easier to handle for measurement of the grids. Figure 9(a) records the replicating set-up and Fig. 9(b) is a photograph showing the quality of replicating the grid pattern. The photoresist technique of surface gridding leaves the grid lines slightly proud of the surface thus giving optical contrast.

As well as direct photography of the grid patterns on each of the four surfaces before any deformation occurred, replicas were also taken. Replicas were also taken of each of the four surfaces at each of the deformed load levels, as detailed above.

5.3 Coordinate system and grid point designations

For purposes of grid measurements, and to achieve consistency of presentation between measurement and any predictions, it is necessary to designate faces and assign coordinate systems. The four faces are simply designated 1 to 4, with faces 2 and 4 being the compression and tension faces respectively, and faces 1 and 3 being the side faces, as illustrated in Fig.10. This figure also gives the coordinate system adopted for each face. When viewing the faces normally the coordinate directions on each face are identical , that is by viewing one face and rotating the specimen around its longitudinal axis, the coordinate directions on any other face appear the same. Therefore the coordinate directions are not spatially absolute; the positive z- and y-directions are opposite on opposite faces.

Figure 11 shows diagrammatically the square grid pattern for measurement and prediction of displacements and the row/column designations. The zero of the coordinate system is located at row 8, column 8, and is thus, nominally, in the centre of each face.

---

* Bayer Xantopren blue dental impression material.

5.4 Grid measurement technique

The 15 by 15 grid intersections for each face were measured semi-automatically with the aim of determining the change in x, y, z coordinates, denoted Δx, Δy, Δz respectively, for each intersection, face, and bending moment. The measuring equipment is illustrated in Fig. 12 and consists of a microscope with micrometer heads for stage translation, an alignment holder, a CCD camera and visual display unit for image observation, and a PC for data logging and manipulation.

The procedure for replica alignment and measurement is as follows. The replica, still in its casting holder, is mounted on the alignment holder which sits on the microscope translation stage. The alignment holder is capable of rotation and tilt with respect to the optical axis of the microscope. Correct alignment is obtained when the x- and y-directions on the replica coincide with the directions of the translation stage, and the z-direction coincides with the optical axis of the microscope.

The practicalities of alignment rely on the two planes of bending symmetry in the specimen, the normal of one plane being the x-direction as denoted in Fig. 10, the other plane normal being the z-direction of faces 1 or 3, both planes being located through the centre of the specimen, one longitudinal, the other transverse. Because of x-normal symmetry the plan view of the y-axis of the replica, for any face, should remain a straight line even after deformation, and hence column 8 is aligned with one of the translation stage directions by rotation of the alignment holder. This procedure automatically sets the x-direction by virtue of the manufacture of the microscope translation stage. On faces 2 and 4, because of the z-normal (faces 1 and 3) symmetry, the plan view of row 8 also remains a straight line and orthogonal to column 8 and can also be used for x- and y-alignment. On faces 1 and 3, however, the x, y alignment can only be done with column 8.

Alignment of the z-direction with the optical axis of the microscope, for faces 2 and 4, uses both x- and z-normal (faces 1 and 3) symmetry. The intersection of row 8 and column 8 is then either a surface maximum, minimum, or saddle point, and, for a line of any direction passing through this point, the z-displacements at equal distances either side of the point will be equal. Thus, by tilting the alignment holder about two axes, the z-displacements can be made equal at the four corners of the 15 by 15 grid, or at, say, the extremities of row 8 or of column 8. In practice, Δz values for row 8 and column 8 (and often for neighbouring rows and columns) were plotted for the various coordinate positions, and tilts were made to ensure that these plots were as symmetrical as could be obtained about the row 8 / column 8 intersection – see, for example, Fig. 13. That is, all of the z-displacements along both x and y axes were used for alignment, not just the four corner points or the extremities of row or column 8.

The z-direction alignment for faces 1 and 3 is not such a simple matter given that there is only x-normal symmetry. This symmetry allows partial alignment, and by tilting the alignment holder the z-displacements are made equal at equivalent intersections along columns spaced equally from the coordinate zero, say columns 1 and 15. But there is no *a priori* reason why, for faces 1 and 3, the compression and tension deformations should be equal or be of the same sign. That is, if the replica is tilted about the axis of row 8

such that, say, the z-displacements at the extremities of column 8 are equal, it does not necessarily follow that the surface normal at coordinate zero (row 8 / column 8 intersection) is coincident with the optical axis of the microscope. The practical procedure is, again, to use plots of Δz against coordinate position to guide the tilting. Tilting about the y-axis enables symmetry to be achieved between columns equidistant from the coordinate zero. Tilting about the x-axis allows the local region around the coordinate zero to be constant in Δz which is the criterion for the surface normal and the optical axis to be coincident – see, for example, Fig. 13.

Distances in the x- and y-directions are determined from the respective micrometer heads. These heads have a digital output which is logged directly into the PC; they have a reading accuracy of 1 micrometre, and, given the grid and replication quality, the accuracy of measurement is assessed as being ±1 micrometre. Distances in the z-direction are measured by employing the focusing knobs of the microscope which also are calibrated in increments of 1 micrometre. The z-distances are manually entered into the PC and are assessed as having an accuracy of better than ±5 micrometres. Plastic bending of the specimen caused local rumpling which is more pronounced at the higher bending moment. In the rumpled regions the z-distances were measured less accurately than in other regions.

It is obvious from the above that the x- and y-readings are taken with no allowance for curvature. That is, the measurements lead to values of Δx and Δy projected onto the original (undeformed) x-y plane. Values of Δz are distances measured from this plane.

5.5 Displacement predictions

To compare with the experimental results, any predictions of the deformations must list the displacements, Δx, Δy, and Δz, with reference to the undeformed x-y plane, for each of the 15 by 15 grid intersection points. The undeformed grid spacing is to be taken as exactly 2 mm, with the 15 by 15 pattern on each face located centrally and the x-coordinate parallel to the longitudinal axis of the specimen. These predictions are to be made for each of the four faces of the specimen with undeformed dimensions as shown in Fig. 5 (that is, with the square section dimension equal to 29.98 mm), and for both load levels applied during the replication periods (that is -89.5 kN and -92.6 kN).

Obviously, because of symmetries, predictions need cover only about one-quarter of the grid intersection points on faces 2 and 4, and about one-half of the points on either of faces 1 and 3. The displacements predicted are to be for the metal specimen; the replica work described above was a means only of determining metal behaviour, and the results given in Part II have been converted to metal displacements.

Table 6 shows the tabular format of the results that is used in Part II. If predictors wish the authors to compare the predictions with experiment, the information should be stored as a text file on a 3.5 inch diskette readable by MS DOS.

ACKNOWLEDGEMENT

The contribution of Dr P.W. Beaver early in this project is gratefully acknowledged.

REFERENCES

1. Ramberg,W. and Osgood,W.R. Description of stress - strain curves by three parameters. N.A.C.A. Tech. Note no.902, July 1943.

2. Kowal,E.A.B. A microgrid procedure for local strain measurements. DSTO ARL-TN- (in preparation).

Table 1. Tensile properties in longitudinal direction of 7050-T7451 aluminium alloy

(a) determined by manufacturer

Number of Tests	Ultimate Strength (MPa)	Yield Strength (MPa)	Elongation (%)
2	532, 533	480, 481	10.5, 10.5

(b) determined in present work

0.1% Proof Stress (MPa)	481.5
0.2% Proof Stress (MPa)	489.0

Table 2. Experimental stress-strain data (average of two specimens)

Stress (MPa)	Strain (%)
0.00	0.00
85.22	0.12
165.22	0.23
237.65	0.33
320.64	0.46
396.14	0.58
445.66	0.67
466.33	0.72
477.90	0.76
483.01	0.79
487.23	0.85
490.08	0.93
492.03	1.01
494.03	1.14
496.87	1.40
500.10	1.75
504.91	2.23
512.03	3.02
517.38	3.67
523.09	4.46
527.08	5.24
529.62	6.05
531.07	6.87
532.89	7.93
532.16	9.15
530.71	10.14
529.26	10.99
526.36	12.02

Table 3. Stress relaxation properties of 7050-T7451 aluminium alloy plate

(a) nominal tensile strain 0.04

Time (minutes)	Stress (MPa)		
	Specimen KD1G2	Specimen KD1G12	Specimen KD1G6
0.02	516.5	509.3	505.2
0.08	508.3	501.9	496.9
0.17	505.0	498.1	495.3
0.25	503.3	496.5	491.2
0.33	500.0	494.9	490.4
0.42	499.2	492.4	488.8
0.50	496.7	491.2	487.5
0.58	495.9	490.4	486.3
0.66	495.9	489.9	485.9
0.75	495.5	489.9	484.6
0.83	495.1	487.9	483.8
0.92	494.2	487.9	483.0
1.00	493.5	487.5	482.6
1.17	492.6	486.3	482.2
1.33	491.8	485.5	481.3
1.50	490.9	483.8	480.5
1.66	490.2	483.0	478.9
1.83	489.7	483.0	478.0
2.00	489.3	482.3	477.3
2.50	487.7	479.7	476.3
3.00	485.2	478.4	475.6
3.50	484.4	477.6	474.8
4.00	484.0	477.3	473.5
4.50	483.1	476.0	472.3
5.00	481.9	475.6	471.1
5.50	481.1	475.1	470.7
6.00	480.3	474.8	470.2
6.50	479.4	474.4	469.4
7.00	479.0	473.5	468.6
7.50	478.6	472.3	468.6
8.00	477.8	471.1	468.2
8.50	477.0	471.1	467.8
9.00	476.5	470.7	467.4
15	472.0	466.5	465.8
21	470.4	463.3	463.6
27	467.9	462.5	461.2
33	466.2	460.0	460.0
39	463.8	457.9	457.3
45	462.2	455.4	456.7
51	461.7	457.1	455.4
57	461.3	455.4	454.6
63	460.5	454.6	454.3
69	459.8	453.4	453.4
75	459.3	453.4	
81	458.4	453.0	

continued

Table 3 (a) continued

Time (minutes)	Stress (MPa)		
	Specimen KD1G2	Specimen KD1G12	Specimen KD1G6
87	457.2	452.1	
93	457.2	451.8	
99	456.7	451.0	
105	455.6	450.1	
111	455.1	449.3	
117	454.7	448.5	
123	454.3	447.7	
129	453.9		
135	453.5		
141	453.1		
147	452.7		
153	452.7		
159	452.7		
165	452.3		
171	451.8		
177	451.4		
183	451.0		
189	450.2		
195	449.8		
201	449.4		
207	449.0		
213	449.0		
219	448.5		
225	448.1		
231	447.7		
237	447.7		
243	447.7		
249	447.7		
255	447.3		
261	446.9		
267	446.5		
300	445.2		
330	444.4		
360	444.0		

Table 3. Stress relaxation properties of 7050-T7451 aluminium alloy plate

(b) nominal tensile strain 0.08

Time (minutes)	Stress (MPa)	
	Specimen KD1G6	Specimen KD1G12
0.02	517.5	521.6
0.08	509.3	510.5
0.17	503.5	506.4
0.25	499.8	502.7
0.33	497.8	499.4
0.42	495.3	497.8
0.50	494.5	496.5
0.58	492.0	494.5
0.66	491.2	493.6
0.75	490.9	492.0
0.83	490.4	491.2
0.92	489.5	490.4
1.00	487.9	489.9
1.17	486.3	487.9
1.33	485.5	486.3
1.50	484.6	485.5
1.66	483.0	485.0
1.83	482.2	483.4
2.00	481.7	483.0
2.50	478.9	479.7
3.00	476.4	478.0
3.50	475.6	477.3
4.00	474.8	475.6
4.50	474.0	475.1
5.00	472.3	473.5
5.50	470.7	472.3
6.00	469.8	471.1
6.50	469.4	470.7
7.00	469.0	469.8
7.50	468.2	469.0
8.00	467.4	468.6
8.50	466.9	467.4
9.00	466.5	467.4
15	461.6	
21	457.5	
27	455.0	
33	453.4	
39	451.0	
45	449.3	
51	447.7	
57	446.0	
63	446.2	
69	445.2	
75	444.4	
81	443.5	

continued

Table 3 (b) continued

Time (minutes)	Stress (MPa)	
	Specimen KD1G6	Specimen KD1G12
87	442.8	
93	441.9	
99	441.1	
105	440.3	
111	439.5	
117	440.1	
123	439.5	
129	439.0	
135	438.6	
141	437.8	
147	437.8	
153	437.8	
159	437.4	
165	437.0	
171	436.6	
177	436.6	
183	435.3	
189	435.3	
195	434.5	
201	434.5	
207	434.5	
213	434.5	
219	433.7	
225	433.7	
231	432.9	
237	432.9	
243	432.9	
249	432.9	
255	432.0	
261	432.0	
267	431.3	
300	429.6	
330	428.3	
360	427.1	
390	425.5	
420	425.5	
450	425.5	
480	424.7	
510	424.7	
540	423.0	
570	421.4	
600	423.0	
630	421.3	
660	420.7	
690	421.8	
720	418.1	
750	418.1	
780	418.1	

continued

Table 3 (b) continued

Time (minutes)	Stress (MPa)	
	Specimen KD1G6	Specimen KD1G12
810	418.1	
840	418.1	
870	417.3	
900	417.3	
930	417.3	
960	416.5	
990	416.5	
1020	416.5	
1050	414.8	
1080	414.8	
1110	414.0	

Table 3. Stress relaxation properties of 7050-T7451 aluminium alloy plate

(c) nominal tensile strain 0.12

Time (minutes)	Stress (MPa)			
	Specimen KD1G10	Specimen KD1G6	Specimen KD1G12	Specimen KD1G3
0.02	502.3	506.8	511.3	522.7
0.08	492.8	495.3	500.6	506.3
0.17	487.5	490.4	495.3	499.8
0.25	483.4	487.9	491.6	496.5
0.33	481.7	486.3	490.8	493.9
0.42	479.7	483.8	488.3	492.6
0.50	478.4	481.3	486.6	491.3
0.58	477.3	480.5	486.3	489.4
0.66	475.1	478.4	484.2	488.0
0.75	474.0	478.0	483.4	487.4
0.83	473.1	477.3	483.0	484.8
0.92	472.3	475.6	482.6	484.1
1.00	471.5	475.1	480.5	483.5
1.17	469.8	474.8	478.9	482.2
1.33	469.0	473.5	478.0	480.2
1.50	466.9	472.7	476.4	479.6
1.66	466.5	471.1	475.6	478.9
1.83	466.1	469.8	474.8	476.3
2.00	465.3	469.0	474.4	476.3
2.50	462.5	466.5	471.9	473.0
3.00	460.4	464.9	469.8	471.7
3.50	459.2	462.9	469.4	469.8
4.00	457.5	462.5	467.4	467.8
4.50	456.3	461.6	465.8	467.1
5.00	455.0	460.0	464.9	466.5
5.50	454.3	459.2	462.5	465.2
6.00	452.1	458.3	462.5	463.9
6.50	450.1	457.5	461.6	463.4
7.00	449.5	456.7	461.2	462.6
7.50	449.3	455.0	460.0	461.8
8.00	448.5	454.3	459.2	461.1
8.50	447.7	454.3	458.3	460.4
9.00	446.0	453.4	457.9	460.0
15	441.9	448.5		
21	440.3	445.2		
27	437.4	441.9		
33	435.3	437.8		
39	434.5	437.0		
45	433.7	437.0		
51	432.0	435.3		
57	430.4	434.1		
63	429.2	432.0		
69	428.8	432.0		
75	426.3	431.3		
81	425.1	429.6		

continued

Table 3 (c) continued

Time (minutes)	Stress (MPa)			
	Specimen KD1G10	Specimen KD1G6	Specimen KD1G12	Specimen KD1G3
87	424.7	428.8		
93	423.8	428 4		
99	423.0	428.0		
105	422.2	428.0		
111	421.4	426.7		
117	420.5	425.5		
123	420.5	424.7		
129	419.8			
135	419.3			
141	418.1			
147	417.3			
153	416.9			
159	416.5			

Table 4. Polynomial best-fit coefficients for stress relaxation of 7050-T7451 aluminium alloy plate

$$\text{Stress (MPa)} = a + b \log_{10}[\text{time(minutes)}] + c \log_{10}[\text{time(minutes)}]^2$$

Nominal Strain	Specimen Number	Polynomial Coefficients		
		a	b	c
0.04	KD1G2	493.419	-15.7861	-1.41180
	KD1G6	482.590	-14.7506	-0.58384
	KD1G12	487.006	-15.5682	-1.38664
	Av.	487.672	-15.3683	-1.12743
0.08	KD1G6	487.454	-20.8112	-1.01270
	KD1G12	489.556	-21.9139	-1.79156
	Av.	488.505	-21.3626	-1.40213
0.12	KD1G3	483.238	-23.7869	-0.80403
	KD1G6	475.389	-21.0385	-1.49201
	KD1G10	470.924	-21.6515	-1.23745
	KD1G12	480.653	-21.4525	-2.27794
	Av.	477.551	-21.9824	-1.45286

Table 5. Bend test load/time data

Strain Ramp			Replication	
Ramp order	Elapsed time applied (hour)	Maximum load achieved (at end of ramp and before relaxation) (kN)	Elapsed time commenced (hour)	Load during replication period (kN)
first	zero	-91.2	22	-89.5
second	24	-98.3	46	-92.6

Table 6. Prediction reporting format

(a) Δ x (mm)
(i) steady load = - 89.5kN

Row	Column	Δ x (mm)		
		Face 1*	Face 2	Face 4
1	1	#.###	#.###	#.###
1	2	#.###	#.###	#.###
1	3	#.###	#.###	#.###
1	4	#.###	#.###	#.###
1	5	#.###	#.###	#.###
1	6	#.###	#.###	#.###
1	7	#.###	#.###	#.###
1	8	#.###	#.###	#.###
2	1	#.###	#.###	#.###
2	2	#.###	#.###	#.###
2	3	#.###	#.###	#.###
:	:	:	:	:
:	:	:	:	:
8	7	#.###	#.###	#.###
8	8	#.###	#.###	#.###
9	1	#.###		
9	2	#.###		
:	:	:		
:	:	:		
15	6	#.###		
15	7	#.###		
15	8	#.###		

* Predicted Face 1 and Face 3 displacements are equal;
results expressed in Face 1 orientation

Same tabular arrangement for each of the other conditions, namely, for :

(a) Δ x(mm)
(ii) steady load = -92.6kN

(b) Δ y (mm)
(i) steady load = -89.5kN

(b) Δ y (mm)
(ii) steady load = -92.6kN

(c) Δ z (mm)
(i) steady load = -89.5kN

(c) Δ z (mm)
(ii) steady load = -92.6kN

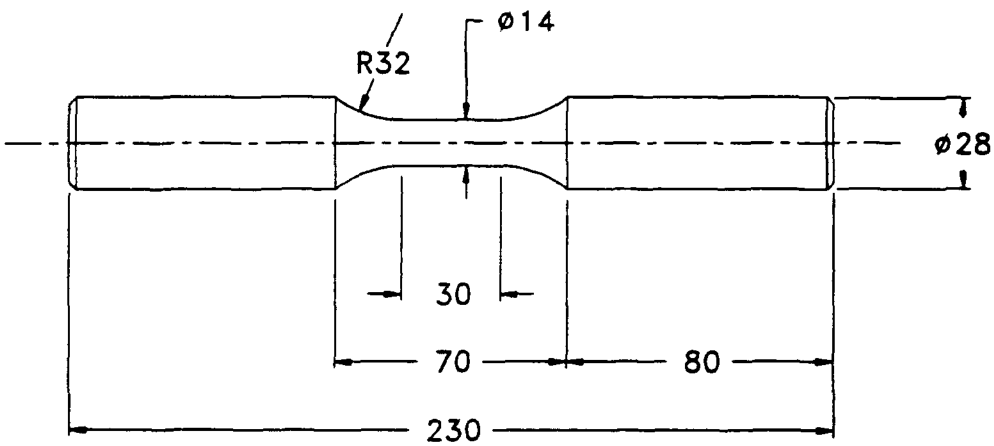

dimensions mm

Fig. 1. Tensile and stress relaxation specimen.

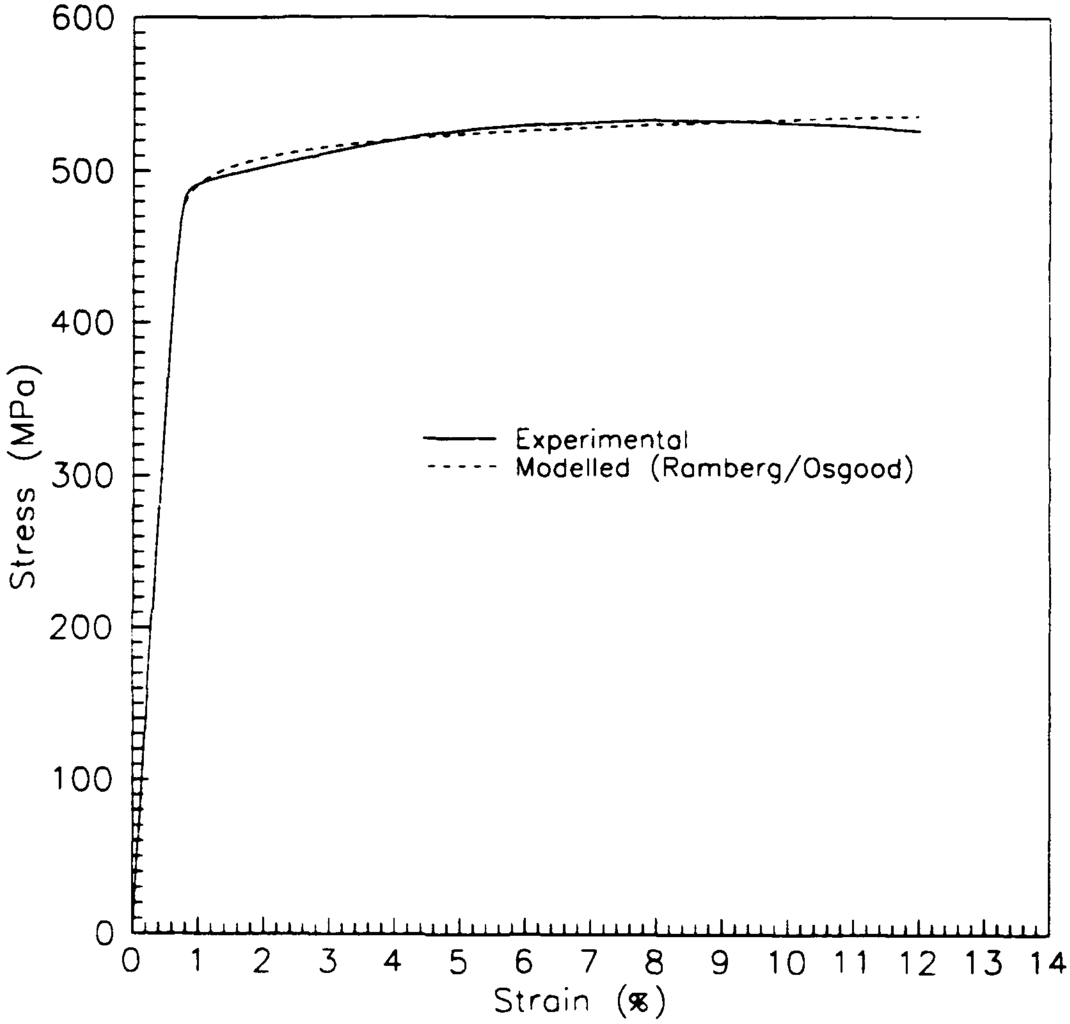

Fig. 2. **Experimental and modelled stress-strain curves 7050-T7451 aluminium alloy.**

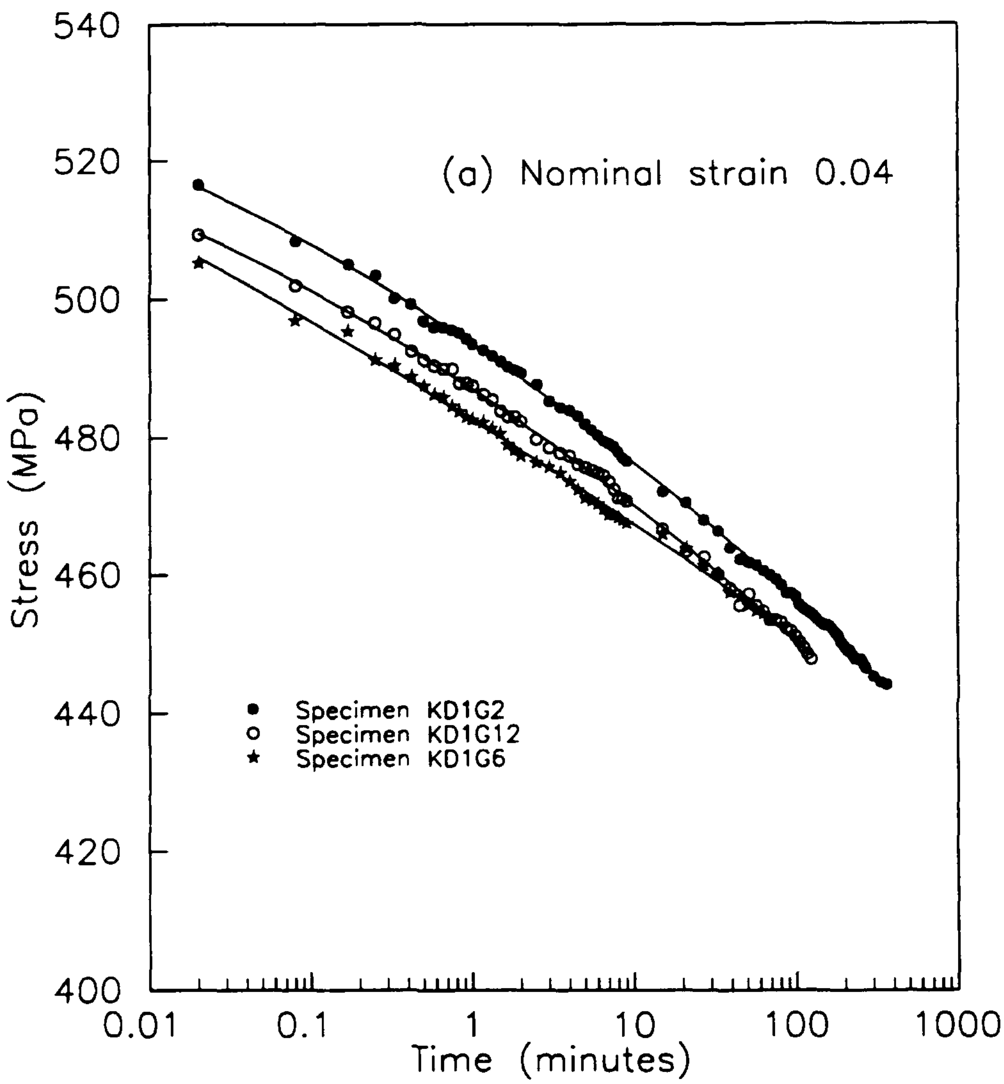

Fig. 3. Stress relaxation of 7050-T7451 aluminium alloy plate.

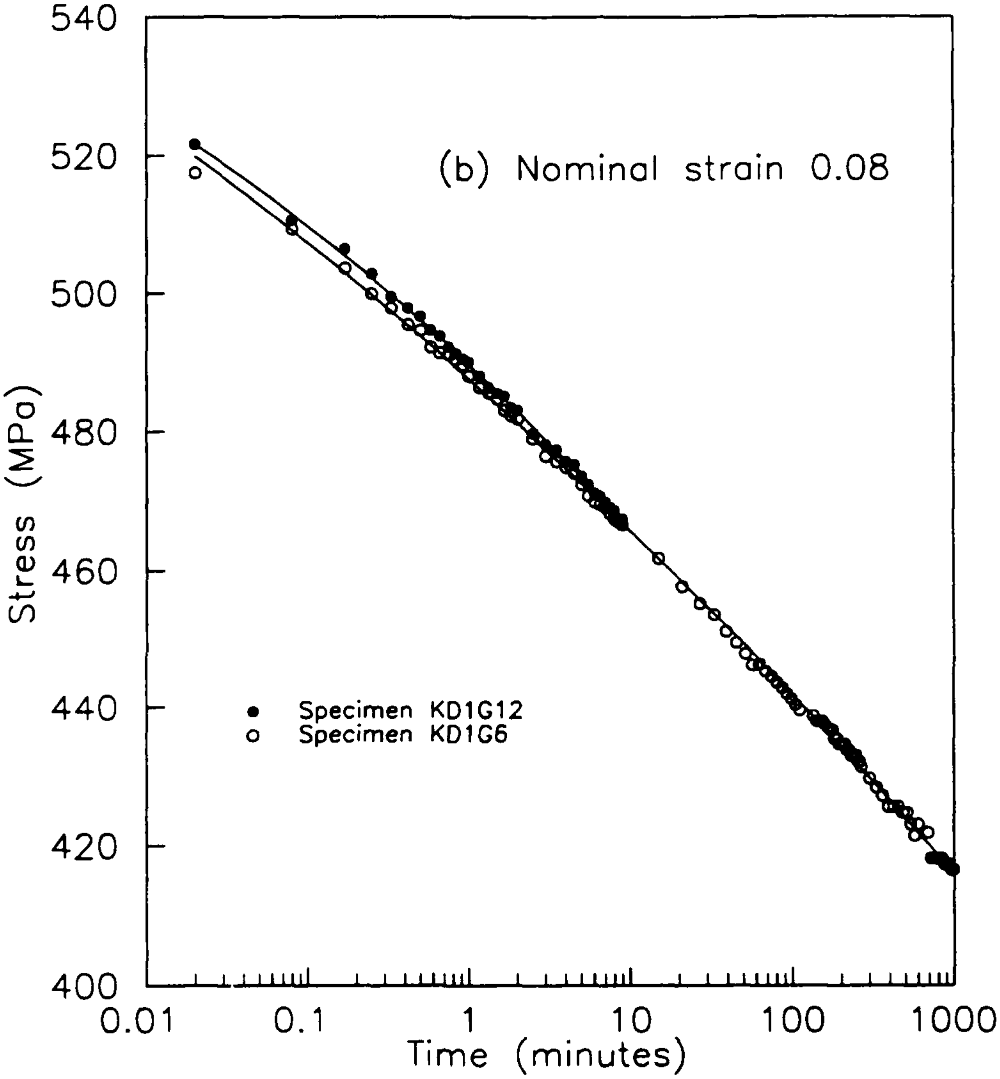

Fig. 3. Stress relaxation of 7050-T7451 aluminium alloy plate.

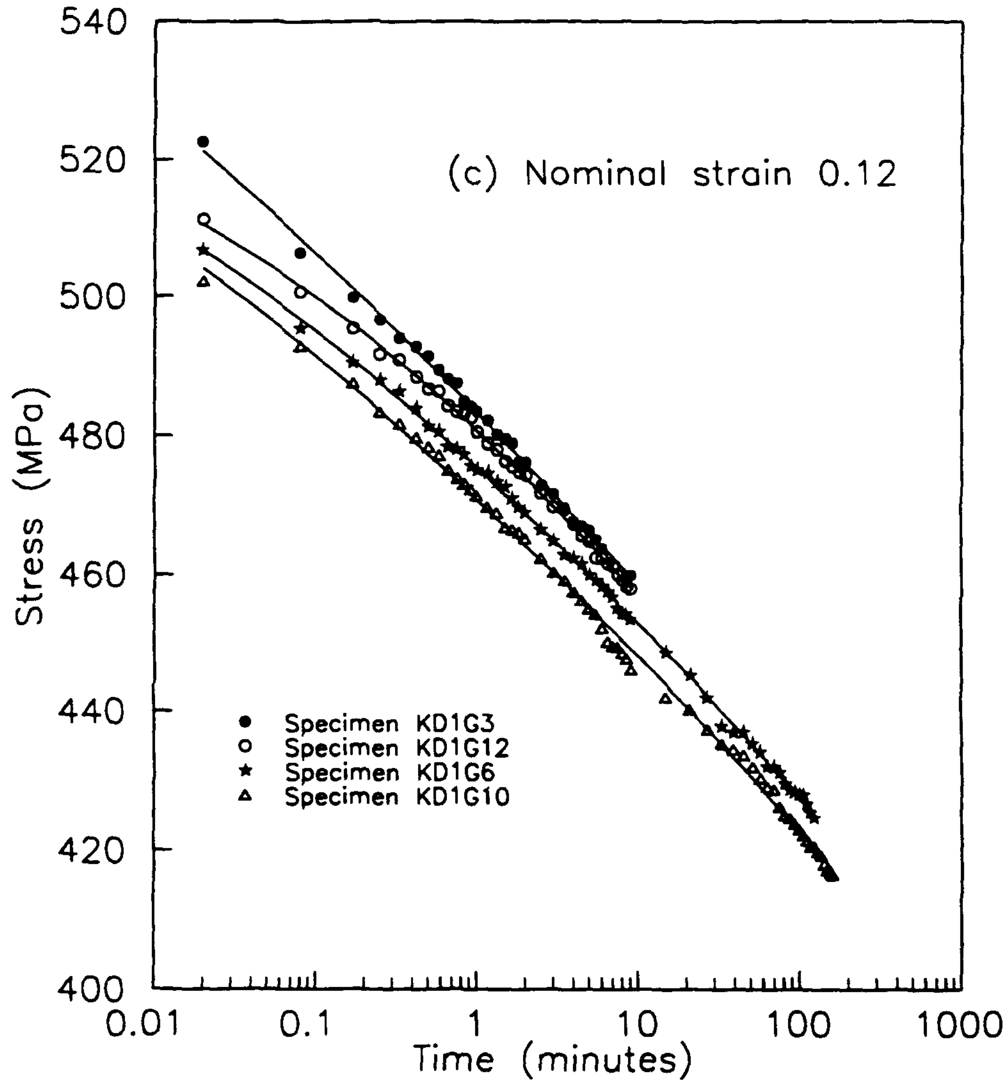

Fig. 3. Stress relaxation of 7050-T7451 aluminium alloy plate.

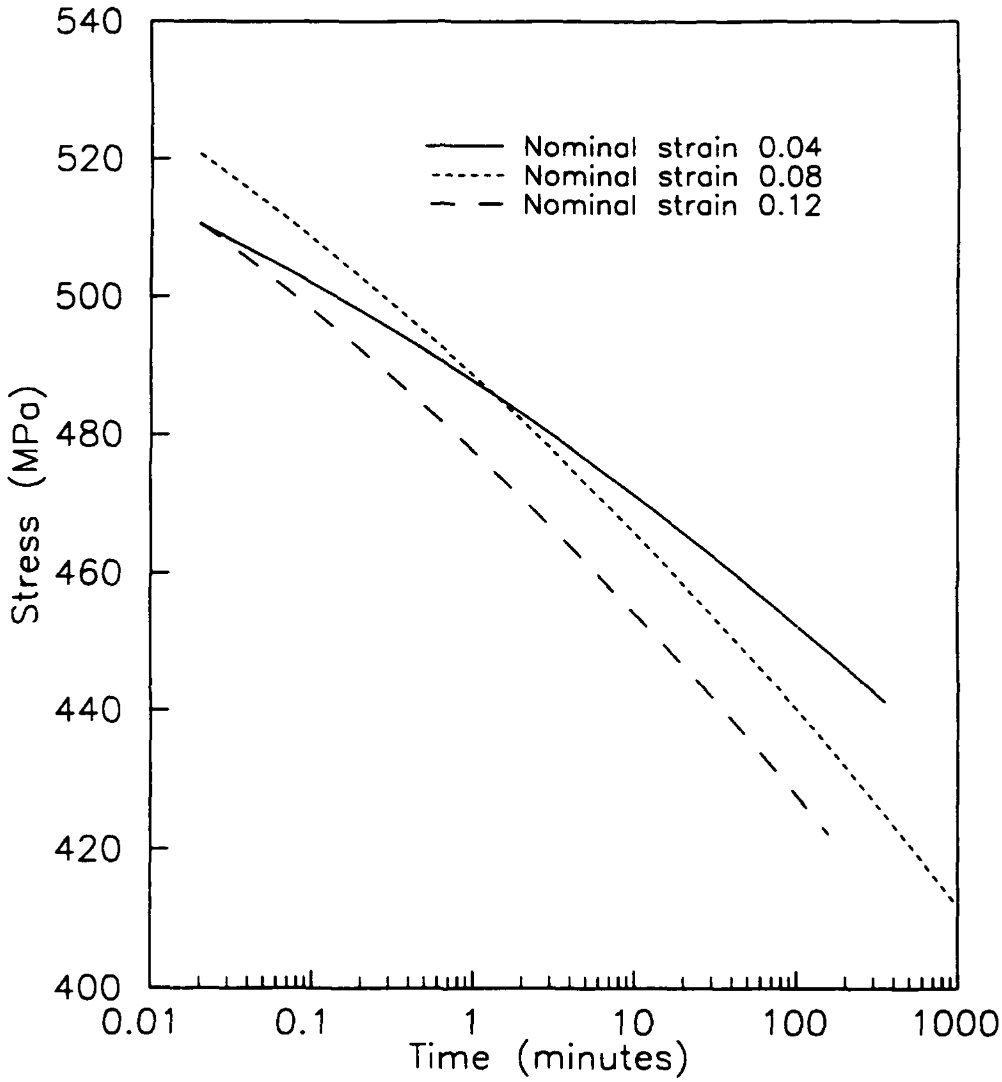

Fig. 4. Average stress relaxation properties of 7050-T7451 aluminium alloy plate.

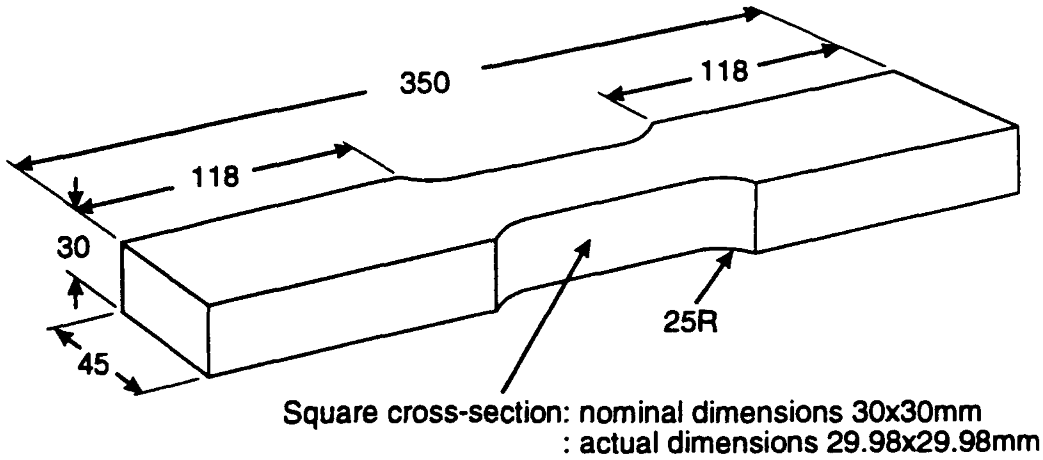

(a) Bending specimen

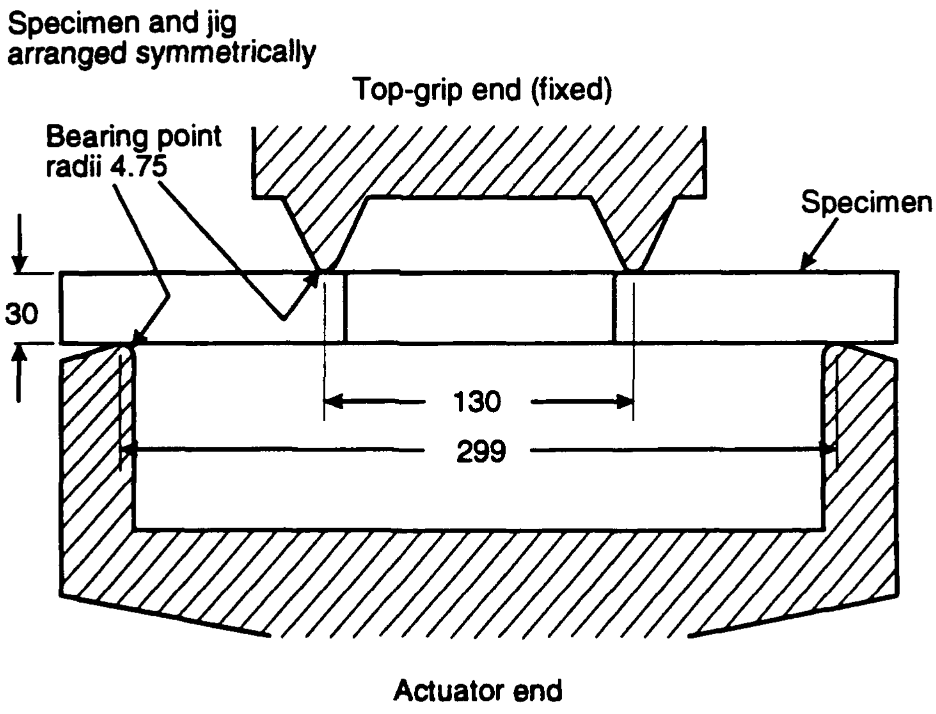

(b) Test jig

Dimensions in mm

Fig. 5. Test arrangement and geometry for 4-point bending specimen.

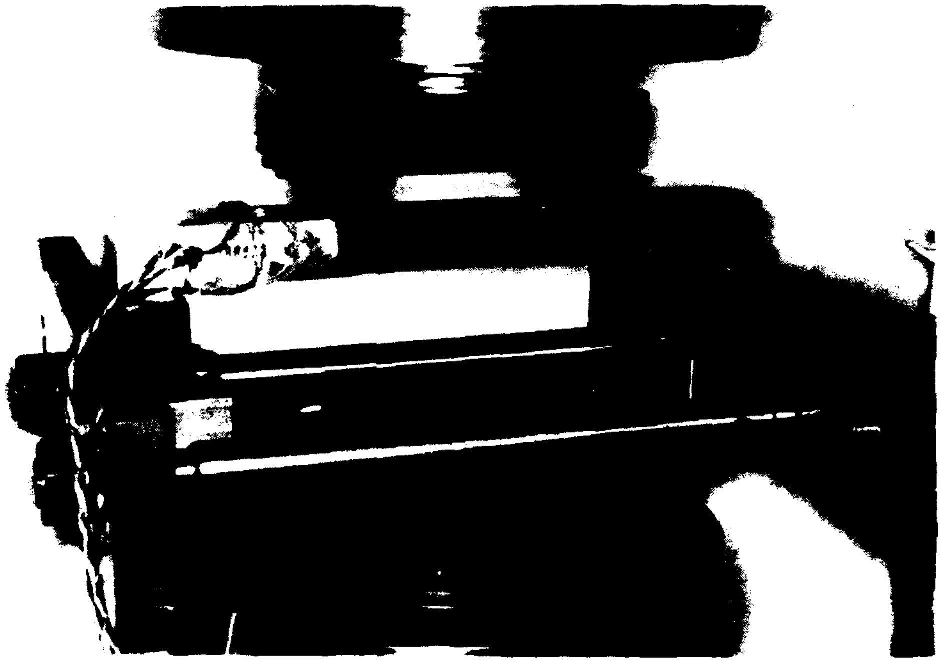

Fig. 6. Bend specimen in 4-point test jig

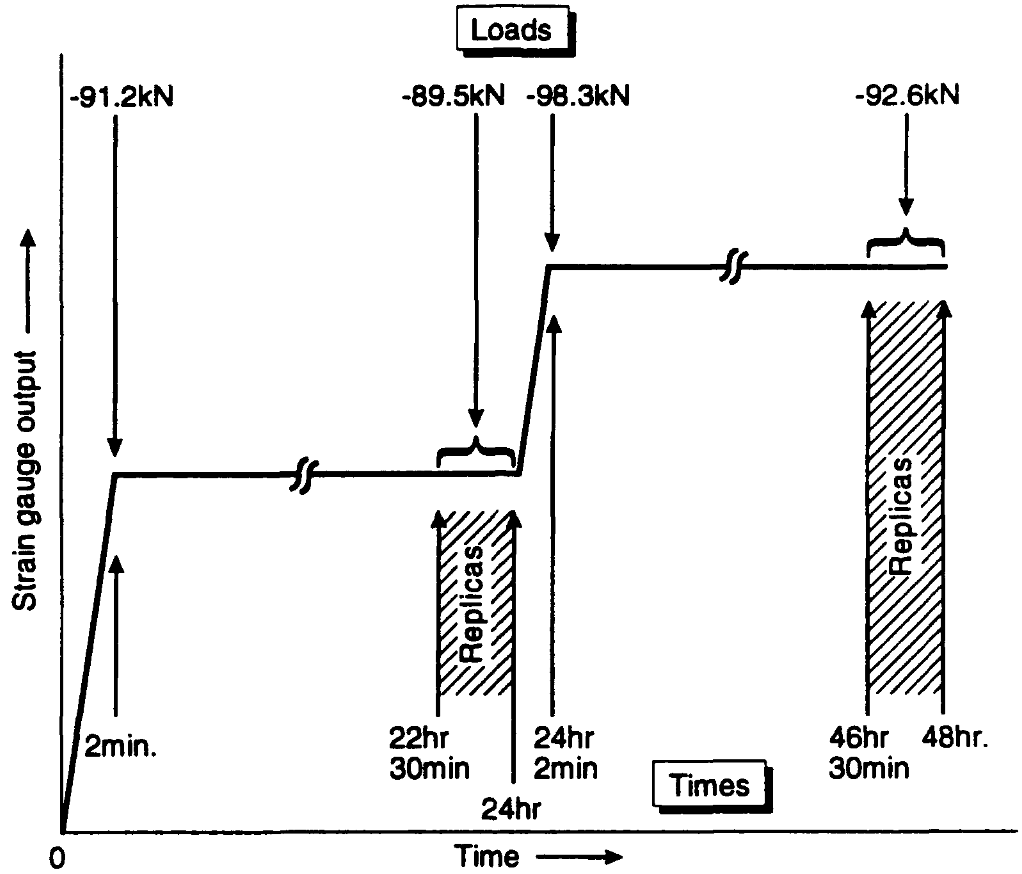

Fig. 7. Bend specimen loading history.

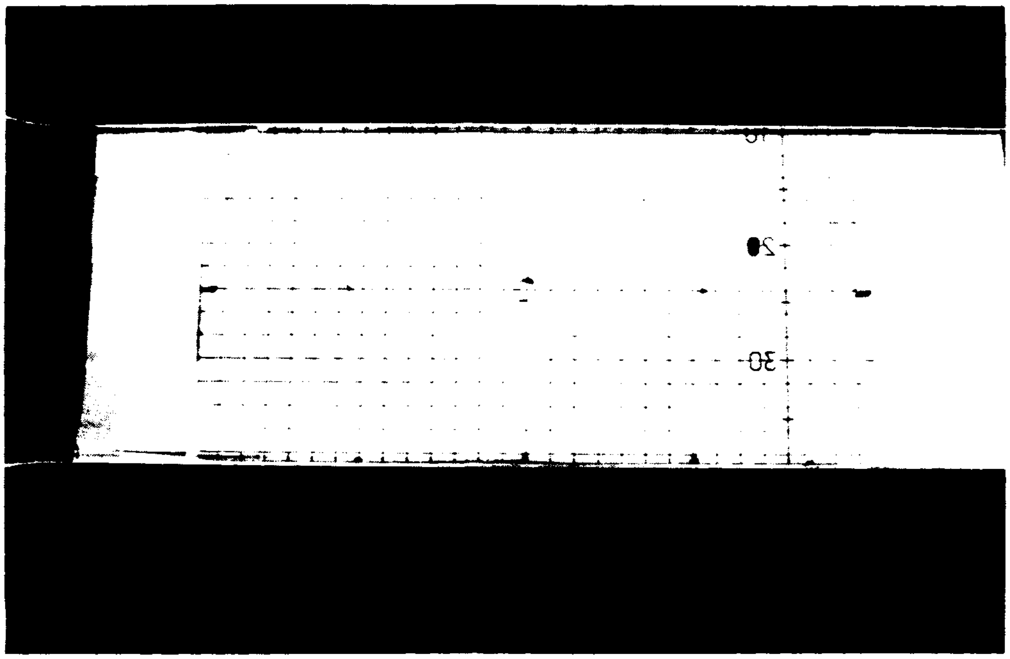

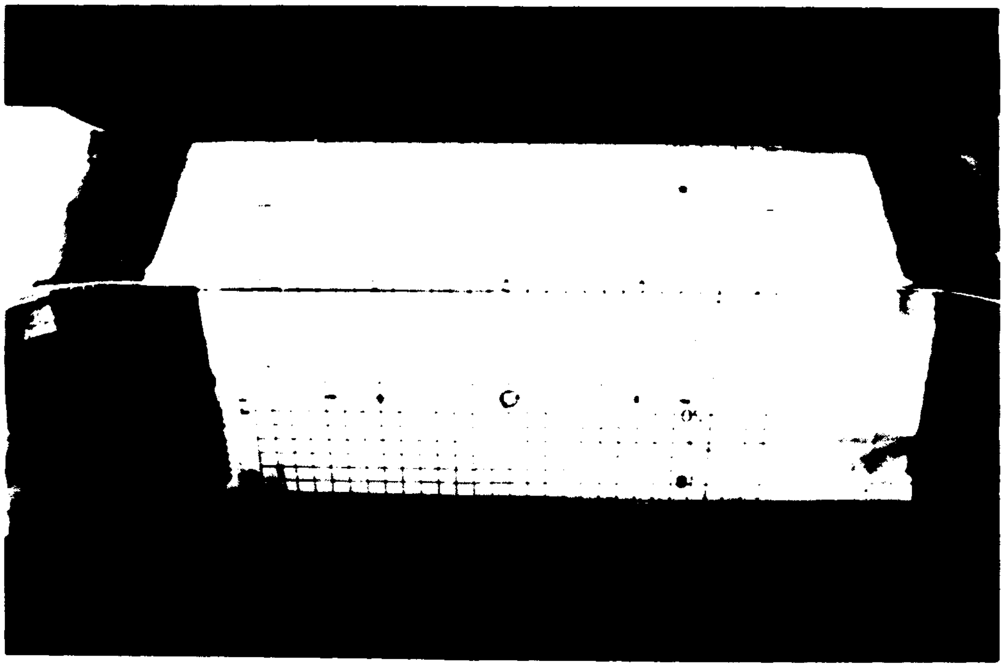

Fig. 8. 2mm square grid pattern on specimen surfaces

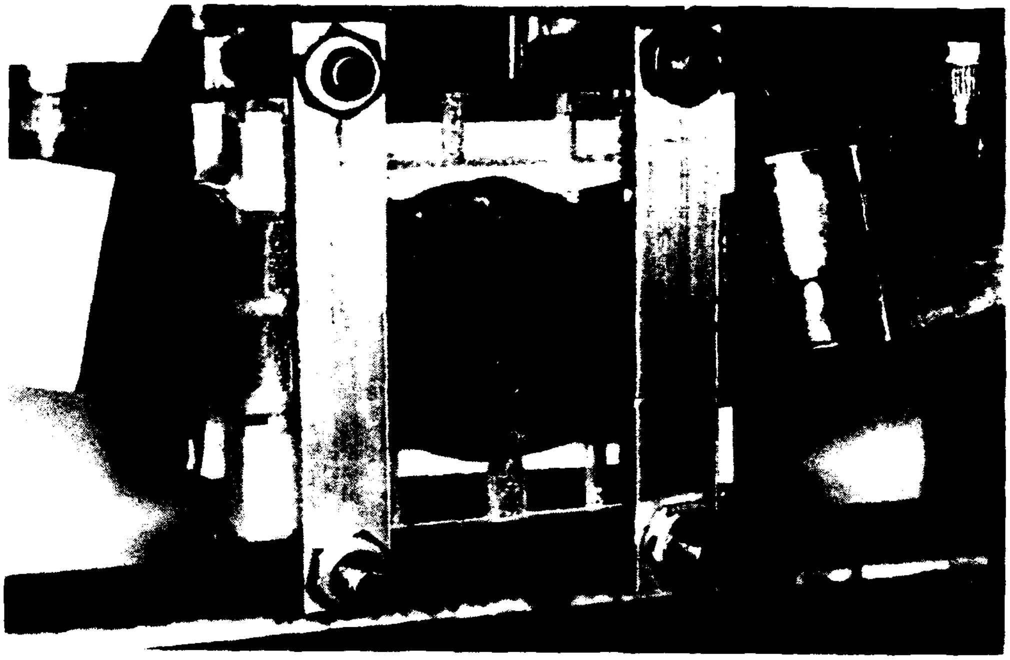

(a) replicating set-up on bend specimen

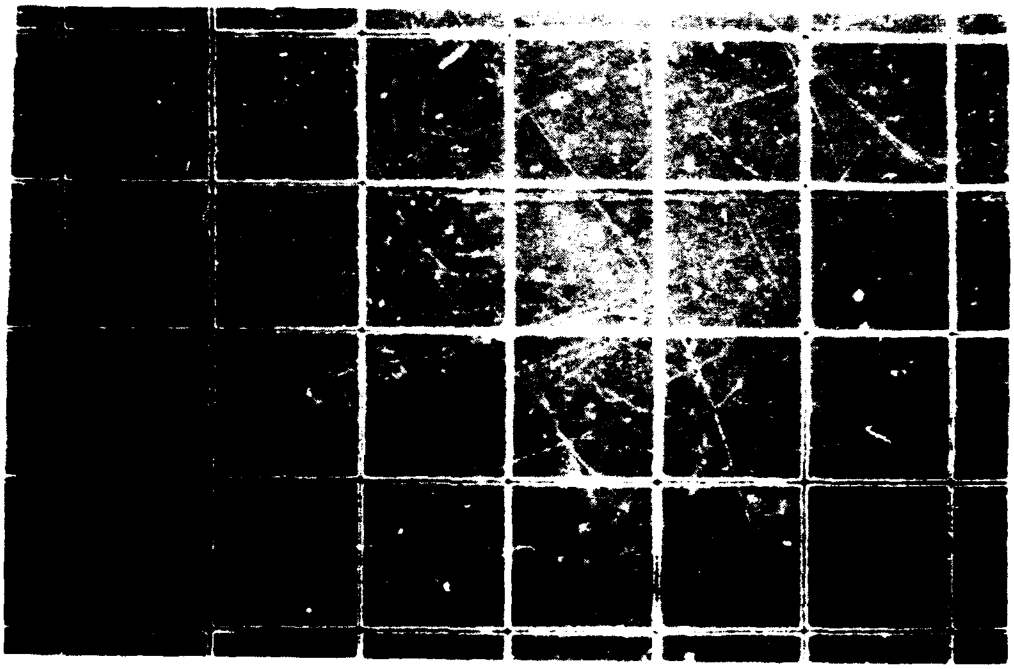

(b) grid pattern on replica

Fig. 9. Replication of photoresist grid pattern

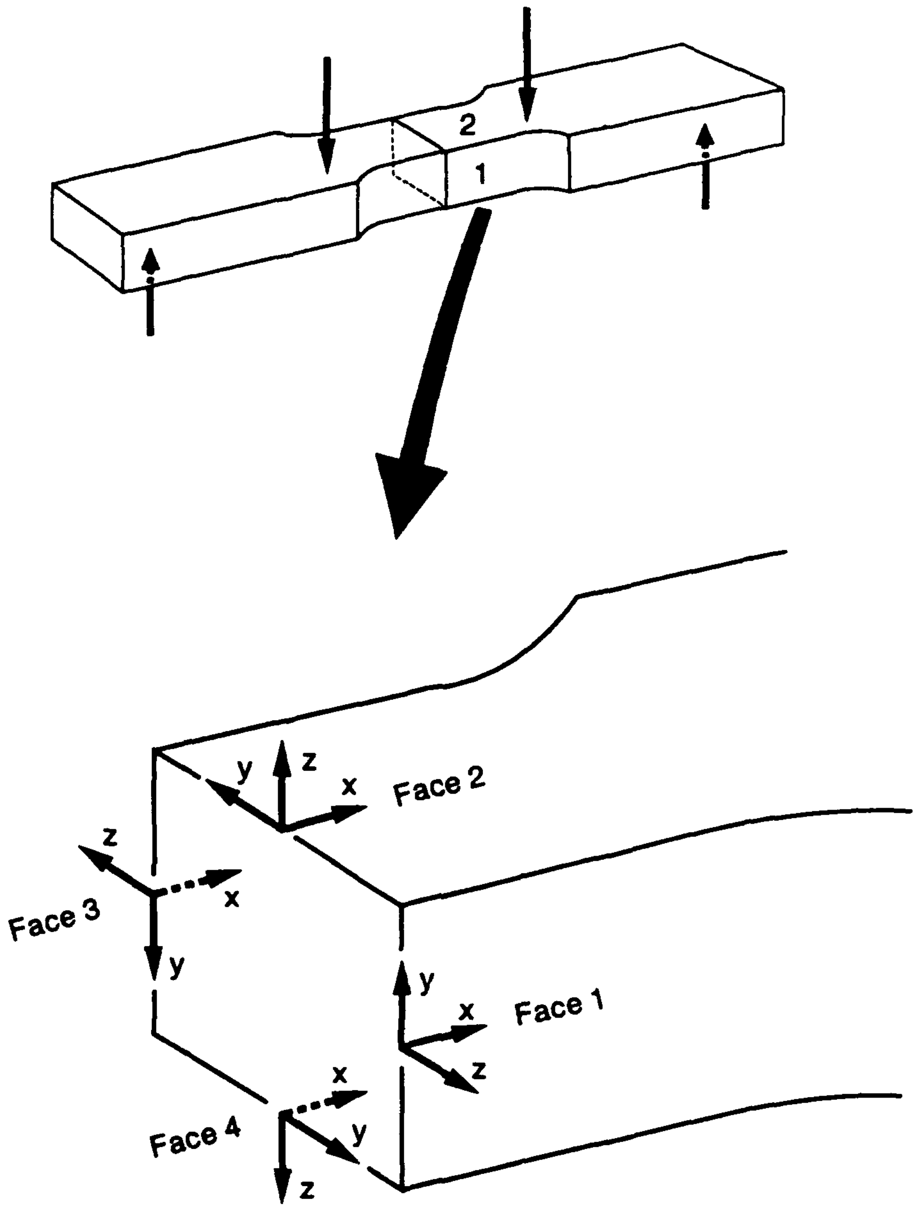

Fig. 10. Specimen face and coordinate designations.

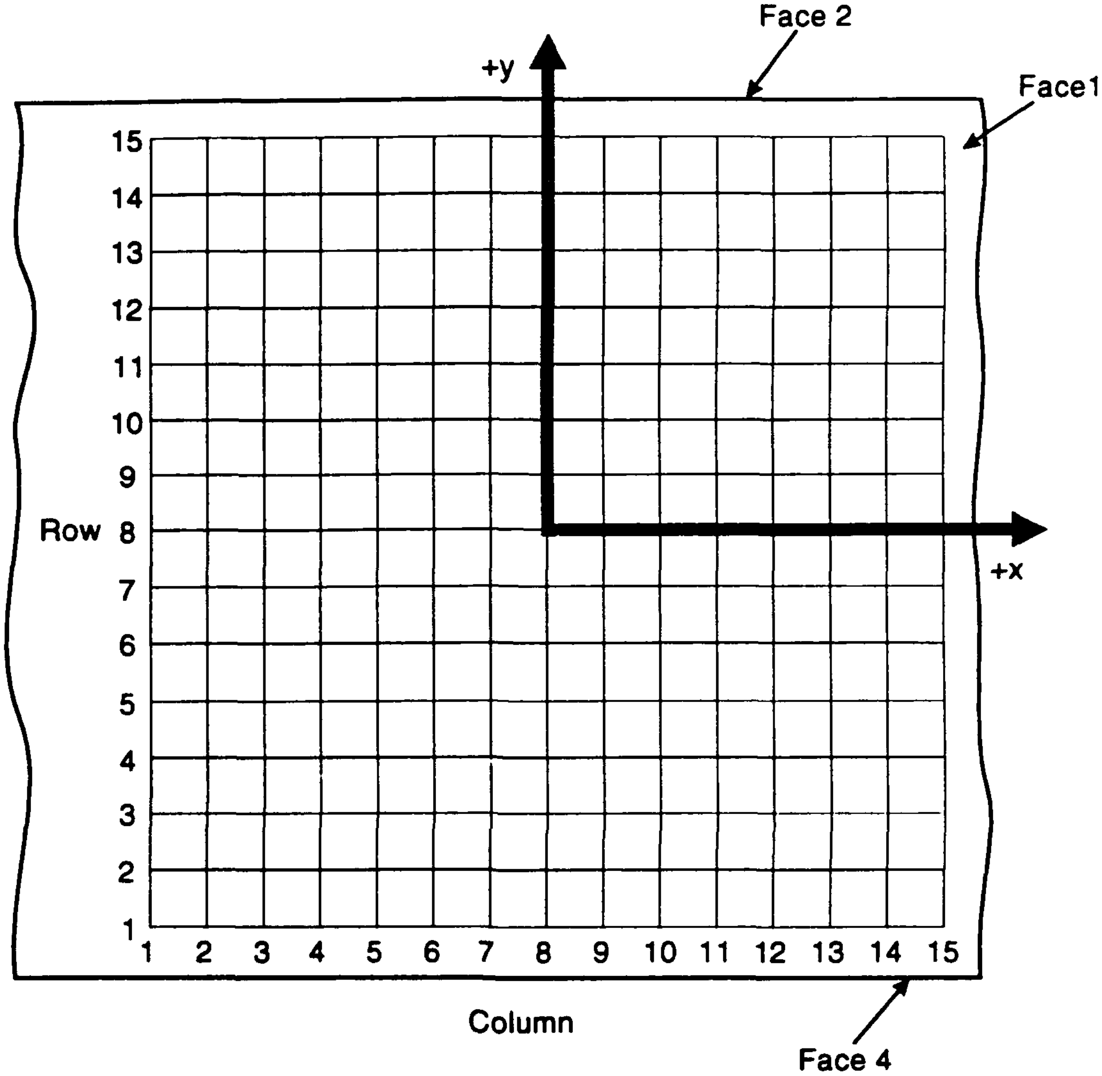

When rotating the specimen about its longitudinal axis, and viewing each face normally, the grid patterns and directions on all faces are identical to those shown.

Fig. 11. Grid coordinate designations.

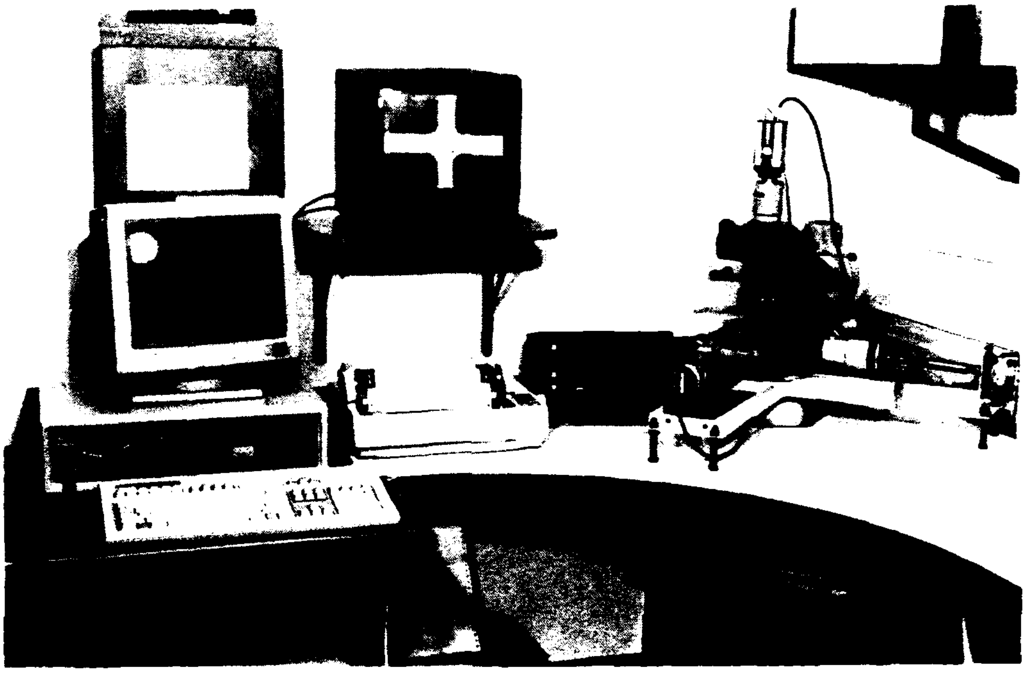

Fig. 12. Grid measuring equipment

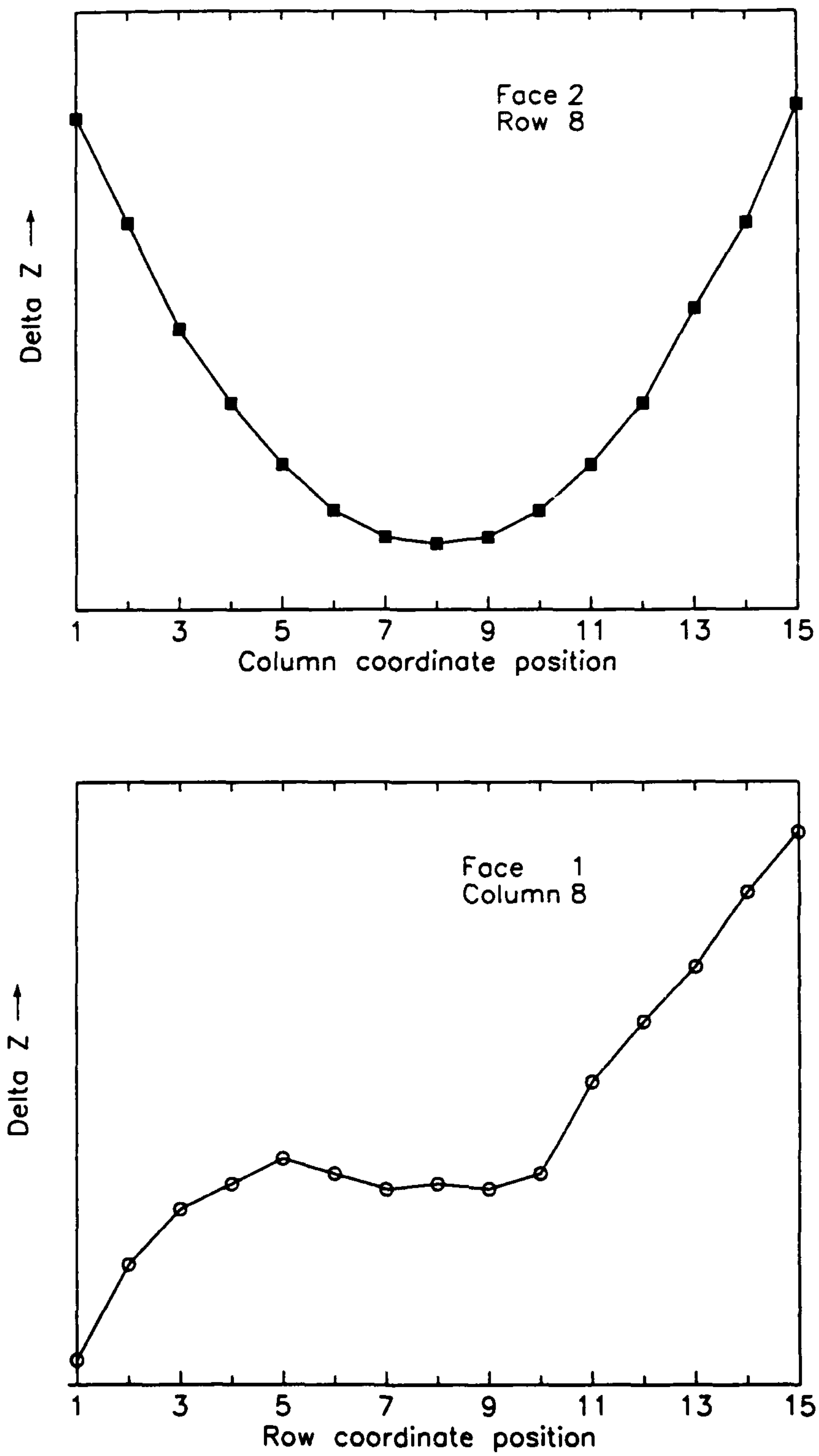

Fig. 13. Z-displacement plots aiding replica alignment. (The points shown here have been inverted in sign to give values appropriate to the metal surface).

DISTRIBUTION

AUSTRALIA

Department of Defence

Defence Central

Chief Defence Scientist
AS, Science Corporate Management
FAS Science Policy
shared copy

Counsellor, Defence Science, London (Doc Data sheet only)
Counsellor, Defence Science, Washington (Doc Data sheet only)
Scientific Adviser, Defence Central
OIC TRS, Defence Central Library
Document Exchange Centre, DSTIC (8 copies)
Defence Intelligence Organisation
Librarian, Defence Signals Directorate, (Doc Data sheet only)

Aeronautical Research Laboratory

Director
Library
Chief Airframes and Engines Division
Authors: J.M. Finney
E.A.B. Kowal
J.G. Sparrow
M. Heller
G.S. Jost

Materials Research Laboratory

Director/Library

Defence Science & Technology Organisation - Salisbury

Library

Navy Office

Navy Scientific Adviser (3 copies Doc Data sheet only)
Director Aircraft Engineering - Navy
Director of Naval Architecture

Army Office

Scientific Adviser - Army (Doc Data sheet only)
Engineering Development Establishment Library
US Army Research, Development and Standardisation Group (3 copies)

Air Force Office

Air Force Scientific Adviser (Doc Data sheet only)
DGELS AIRREG4 HQLC
OIC ATF, ATS, RAAFSTT, WAGGA (2 copies)

Other Organisations

AGPS

Department of Transport & Communication

Library

Statutory and State Authorities and Industry

ASTA Engineering, Document Control Office
Ansett Airlines of Australia, Library
Australian Airlines, Library
Qantas Airways Limited
Civil Aviation Authority
Hawker de Havilland Aust Pty Ltd, Victoria, Library
Hawker de Havilland Aust Pty Ltd, Bankstown, Library
Australian Nuclear Science and Technology Organisation
Gas & Fuel Corporation of Vic., Manager Scientific Services
SEC of Vic., Herman Research Laboratory, Library
BHP, Melbourne Research Laboratories

Universities and Colleges

Adelaide
- Professor Mechanical Engineering

Melbourne
- Engineering Library

Monash
- Hargrave Library
- Head, Materials Engineering
- Prof R. Jones, Mechanical Engineering

Newcastle
- Professor R. Telfer, Institute of Aviation

Sydney
- Engineering Library
- Head, School of Civil Engineering
- Prof Grant Steven, Dept Aeronautical Engineering

NSW
- Physical Sciences Library
- Head, Mechanical Engineering
- Library, Australian Defence Force Academy

Tasmania
Engineering Library

Western Australia
Head, Mechanical Engineering

RMIT
Mr M.L. Scott, Aerospace Engineering

CANADA
CAARC Coordinator Structures

NRC
J.H. Parkin Branch (Aeronautical & Mechanical Engineering Library)

Universities and Colleges
Toronto
Institute for Aerospace Studies

FRANCE
ONERA

GERMANY
Fachinformationszentrum: Energie, Physic, Mathematik GMBH

INDIA
CAARC Coordinator Structures
National Aeronautical Laboratory, Information Centre

INTERNATIONAL COMMITTEE ON AERONAUTICAL FATIGUE
per Australian ICAF Representative (27 copies)

ISRAEL
Technion-Israel Institute of Technology

JAPAN
National Aerospace Laboratory
National Research Institute for Metals, Fatigue Testing Div.

NETHERLANDS
National Aerospace Laboratory (NLR), Library

NEW ZEALAND
Defence Scientific Establishment, Library
RNZAF

Universities

Canterbury

Head, Mechanical Engineering

SINGAPORE

Director, Defence Materials Organisation

SWEDEN

Aeronautical Research Institute, Library

SWITZERLAND

F+W (Swiss Federal Aircraft Factory)

UNITED KINGDOM

Ministry of Defence, Research, Materials and Collaboration

Defence Research Agency (Aerospace)

Farnborough, Head Materials Department

National Physical Laboratory, Library

National Engineering Laboratory, Library

British Library, Document Supply Centre

CAARC Coordinator, Structures

Welding Institute, Library

British Aerospace

Kingston-upon-Thames, Library

Hatfield-Chester Division, Library

Universities and Colleges

Bristol

Engineering Library

Cambridge

Library, Engineering Department

London

Head, Aero Engineering

Manchester

Head, Dept of Engineering (Aeronautical)

Nottingham

Science Library

Southampton

Library

Cranfield Inst. of Technology

Library

Imperial College
Aeronautics Library

UNITED STATES OF AMERICA
NASA Scientific and Technical Information Facility
Boeing Commercial Airplanes
United Technologies Corporation, Library
Lockheed-California Company
Lockheed Georgia
McDonnell Aircraft Company, Library

Universities and Colleges

Florida
Head, Engineering Sciences

Johns Hopkins
Head, Engineering Department

Iowa State
Head, Mechanical Engineering

Princeton
Head, Mechanics Department

Massachusetts Inst. of Technology
MIT Libraries

SPARES (9 COPIES)

TOTAL (140 COPIES)

AL 149 DEPARTMENT OF DEFENCE

PAGE CLASSIFICATION
UNCLASSIFIED

PRIVACY MARKING

DOCUMENT CONTROL DATA

1a. AR NUMBER	1b. ESTABLISHMENT NUMBER	2. DOCUMENT DATE	3. TASK NUMBER
AR-008-363	ARL-RR-6 PART I	JUNE 1993	DST 92/069

4. TITLE	5. SECURITY CLASSIFICATION	6. NO. PAGES	7. NO. REFS.
A BENCHMARK BENDING TEST OF A THICK SPECIMEN PART I - EXPERIMENTS	(PLACE APPROPRIATE CLASSIFICATION IN BOX(S) IE. SECRET (S), CONF. (C) RESTRICTED (R), LIMITED (L), UNCLASSIFIED (U)). Document: U; Title: U; Abstract: U	36	2

8. AUTHOR(S)
J.M. FINNEY
E. KOWAL

9. DOWNGRADING/DELIMITING INSTRUCTIONS
Not applicable.

10. CORPORATE AUTHOR AND ADDRESS
AERONAUTICAL RESEARCH LABORATORY
AIRFRAMES AND ENGINES DIVISION
506 LORIMER STREET
FISHERMENS BEND VIC 3207

11. OFFICE/POSITION RESPONSIBLE FOR:
SPONSOR: DSTO
SECURITY: -
DOWNGRADING: -
APPROVAL: CAED

12. SECONDARY DISTRIBUTION (OF THIS DOCUMENT)

Approved for public release.

OVERSEAS ENQUIRIES OUTSIDE STATED LIMITATIONS SHOULD BE REFERRED THROUGH DSTIC, ADMINISTRATIVE SERVICES BRANCH, DEPARTMENT OF DEFENCE, ANZAC PARK WEST OFFICES, ACT 2601

13a. THIS DOCUMENT MAY BE ANNOUNCED IN CATALOGUES AND AWARENESS SERVICES AVAILABLE TO ....

No limitations.

13b. CITATION FOR OTHER PURPOSES (IE. CASUAL ANNOUNCEMENT) MAY BE [X] UNRESTRICTED OR [ ] AS FOR 13a.

14. DESCRIPTORS		15. DISCAT SUBJECT CATEGORIES
Metals	Aluminum 7050	110601
Plastic properties	Bending	
Plasticity tests	Surfaces	
Benchmarks	Deformation	

16. ABSTRACT
An experiment has been undertaken to provide benchmark data for validating methods of calculating the plastic behaviour of metals. In this experiment a 30 mm square-test-section specimen of 7050-T7451 aluminium alloy has been loaded in four-point bending, and the surface distortions of all four faces have been measured with the aid of a square grid pattern imposed on the surfaces before deformation. This part of the Report describes the experimental details and gives the results of the material property tests, thus providing sufficient information for the prediction of surface displacements. Part II of the Report gives the measured displacements with which predictions may be compared.

PAGE CLASSIFICATION
UNCLASSIFIED

PRIVACY MARKING

THIS PAGE IS TO BE USED TO RECORD INFORMATION WHICH IS REQUIRED BY THE ESTABLISHMENT FOR ITS OWN USE BUT WHICH WILL NOT BE ADDED TO THE DISTIS DATA UNLESS SPECIFICALLY REQUESTED.

16. ABSTRACT (CONT).

17. IMPRINT

AERONAUTICAL RESEARCH LABORATORY, MELBOURNE

18. DOCUMENT SERIES AND NUMBER	19. WA NUMBER	20. TYPE OF REPORT AND PERIOD COVERED
Research Report 6 Part I	21 227C	

21. COMPUTER PROGRAMS USED

22. ESTABLISHMENT FILE REF.(S)

23. ADDITIONAL INFORMATION (AS REQUIRED)